



Title	Effect of Welding Parameters of FCAW Process and Shielding Gas Type on Weld Bead Geometry and Hardness Distribution(Materials, Metallurgy & Weldability)
Author(s)	Sadek, A.; Ibrahim, R. N.; Price, J W H et al.
Citation	Transactions of JWRI. 2001, 30(2), p. 45-52
Version Type	VoR
URL	https://doi.org/10.18910/6162
rights	
Note	

The University of Osaka Institutional Knowledge Archive : OUKA

<https://ir.library.osaka-u.ac.jp/>

The University of Osaka

Effect of Welding Parameters of FCAW Process and Shielding Gas Type on Weld Bead Geometry and Hardness Distribution†

A. Sadek*, R.N.Ibrahim**, J W H Price**, T.Shehata** and M. Ushio***

Abstract

Flux cored arc welding (FCAW) process is characterized with its high deposition rate and productivity. Knowledge and control of the operating parameters in FCAW are essential if high production rates and welds of good quality are to be consistently obtained. These parameters include arc voltage, welding current, electrode stick-out and travel speed. These operating parameters affect the temperature distribution, weld bead geometry, microstructure of heat affected zone (HAZ), hardness and penetration. Very limited experimental data regarding cooling rate after welding, by FCAW process is available in the literature. Thus, in this paper, the cooling rate after welding was measured experimentally, as a function of welding parameters and its effect on HAZ Hardness examined. Penetration is one of the most important factors controlling hot cracking susceptibility especially in the case of welding thick sections. This paper describes an investigation of the effect of operating parameters on the penetration. An empirical formula is developed to estimate the amount of penetration as a function of operating variables.

KEY WORDS: (FCAW) (Weld bead geometry) (Cooling time) (Weld parameters) (HAZ width)

1. Introduction

The development of better welding methods, especially in the field of automatic welding, requires an accurate knowledge of the relationship between various welding parameters. To achieve this, an improved physical understanding of the welding process is needed. Most process modifications result in some kind of change in the processes within the arc and the melt. The nature of these processes depends on the characteristics of the arc, such as current, temperature, and the resulting heat distribution within the arc, which in turn affect the cooling rate of the weldment.

Flux cored arc welding (FCAW) is an arc welding process in which the heat for welding is generated by an arc between a consumable electrode and the work piece. The electrode, a tubular wire that is continuously fed to the weld area, becomes the filler metal as it is consumed. Shielding of the molten weld pool, arc and adjacent areas of the base metal is obtained from the flux contained within the electrode. Additional shielding is normally obtained from an external supply of gas or gas mixture that is fed through the welding gun.

The gas shield must provide full protection, because even a small amount of entrained air such as from a draft, can contaminate the weld deposit.

Knowledge and control of the operating variables in flux cored arc welding are essential if high production rates and welds of good quality are to be consistently obtained. In this research work all of the FCAW process input parameters and their effect on the output parameters are studied experimentally. The input parameters studied are arc voltage, welding current, electrode stick-out (tip to work distance) and travel speed. These operating parameters affect the output parameters such as weld bead geometry, cooling rate, microstructure, hardness and penetration depth.

The cooling rate after welding has a great influence on the microstructure and in turn on the mechanical properties and performance of the weldments. Very limited experimental data regarding cooling rate after welding of plates by FCAW process is available in the literature. In addition, it is often necessary to place a ceiling on the heat input used to weld high strength low alloy steels.

† Received on December 1, 2001

* CMRDI, Cairo, Egypt

** Monash University, Melbourne, Australia

*** Professor

Transactions of JWRI is published by Joining and Welding Research Institute of Osaka University, Ibaraki, Osaka 567-0047, Japan.

Table 1 Chemical composition of base metal

C	Si	Mn	P	S	Cu	Ni	Cr	Mo
0.22	0.55	1.7	0.04	0.03	0.4	0.5	0.3	0.1

Too slow a cooling rate can lead to the formation of a mixture of proeutectoid ferrite and high carbon martensite, which is also, of course, deleterious to mechanical properties. Thus, in this paper, the cooling rates measured experimentally, as a function of welding parameters, are presented and their effects on HAZ hardness are discussed. Penetration is one of the most important factors controlling hot cracking susceptibility. With increasing penetration the susceptibility of hot cracking is increased especially in the case of welding thick sections. Its effect on hot cracking has been considered and investigated in this study. Also, an empirical formula has been developed to estimate the depth of penetration as a function of two easily measurable operating variables, welding travel speed and tip to work distance. This formula is more practical than other empirical formulas, which are function of welding current and voltage. The accuracy of measuring such variables on site is very good.

2. Experimental Procedure

2.1 Material

The base metal used in this experimental work was 12 mm plates of commercially manufactured C-Mn steel. Typical chemical composition of the material used in this experimental work is given in **Table 1**. Basic flux-cored wire, AWS A5.20, E71T-5 H4 was used through out the experimental work, with 1.2 mm. diameter.

2.2 Welding procedure

An automatic FCAW machine using constant voltage direct current electrode positive (DCEP) was adopted in this study of bead on plate welding. The welding parameters are shown in **Table 2**. The base metals were prepared as strips with the dimension of 400 x 100 x 12 mm to study the effect of welding parameters on temperature distribution, microstructure and weld bead geometry.

Pure argon was used as a shielding gas with flow rate of 7-8 l/min in the case of group A and group C. However, in the case of group B, CO₂ gas was used with a flow rate of 10-12 l/min.

A special welding jig (rigid fixture) was designed and fabricated to hold parts in alignment and to ensure accurate fit-up with no need for tack welding. Meanwhile, by using this jig, which restrains the test strips, the hot cracking tendency can be examined. A short arc and

Table 2 Welding parameters

Group	Gas Type	Current A	Voltage V	Travel speed mm/min	Tip to work distance mm
Effect of shielding gas type and welding conditions					
A	Ar	350	29-30	620	23 25 29
B	CO ₂	380	29-30	620	23 25 28
C	Ar	380	29-30	254 600 1000	25
Effect of welding parameter on cooling time					
D	Ar	150	22	703	25
		170			
		190			
		210			
E		150	23	638	25
		170			
		190			
		210			
F		150	24	510	25
		170			
		190			
		210			
G		150	23	380	25
		170			
		190			
		210			
H	150	24	100	25	
	170				
	190				
	210				

flat bead was maintained during welding. The joint was kept fixed until it cooled down. After slag removal, the samples were released from jig.

2.3 Metallographic investigation

All samples were cut transversely for macrostructure investigation. The macrostructure of studied weldments were examined after etching in 5% Nital. Specimen photographs were enlarged and used in weld area measurements and for measuring HAZ width.

2.4 Hardness testing

Hardness was measured across the weldments using a Vickers diamond indenture with a load of 10 Kg.

2.5 Cooling rate measurements

Temperature and cooling rate were measured by inserting, W, W-Rh thermocouple in the weld pool. The measured value were recorded and analysed instantaneously by the

means of Data Taker connected to PC computer.

3. Result and Discussions

3.1 Effect of tip to work distance on weld bead geometry

The weld bead geometry was measured at different tip to work distance at constant heat input. The results are tabulated in **Table 3** and shown in **Fig.1** in case of pure Ar shielding and **Fig.2** in case of pure CO₂ shielding. The photographs of macrostructure are shown in **Fig.3**.

With increasing tip to work distance within the range tested, the bead width increases and the reinforcement and penetration decrease. This phenomenon can be explained as follows; the electrical current enters the electrode wire at the end of the contact tip. At this point the electrode becomes an electrical conductor and passes the current onto the arc. Since the electrode extension is difficult to measure, the distance from the contact tip to the work ("stick-out") is normally used as the stipulated parameter. If the tip-to-work distance is increased (by pulling the welding gun away from the work) the welding current and penetration will be reduced.

The measured values of weld bead dimensions in the case of Ar gas shielding are higher than in the case of CO₂ gas shielding. This can be attributed to the arc efficiency, which can be related to the ionization potential of these gases. This affects the arc shape and pressure as well as the mode of droplet transfer. Moreover, in case of FCAW, the reactions, which occur during arcing between the flux and the shielding gas, have a great effect on the deposition rate, more research is needed to understand this phenomenon.

Weld metal cross sectional area is a very critical parameter in welding design and has critical values, which cannot be exceeded. When the width of the weld bead is much greater than its depth (width>>depth), the probability of finding toe cracking and/or under bead cracking is increased. On the other hand, when the depth is much greater than the weld bead width, the probability of obtaining hot cracking is increased. In the ASME Code and AWS standard, the conventional ratio of width to depth is recommended to be 2:1.

Table 3 Test results

Spec.No.	Penetration depth mm	Width, mm	Reinforcement, mm	Width/depth	HAZ width Mm
A-1	6	10.81	4.69	2.14	2.19
A-2	5	11.88	4.69	2.38	1.92
A-3	4.5	12.73	4.54	2.83	1.78
B-1	4.5	11.39	3.1	2.53	1.45
B-2	5	11.11	3.1	2.22	1.39
B-3	4	9.33	2.93	2.33	1.33
C-1	8	23.6	6.22	2.95	2.70
C-2	6	15.19	5.6	2.53	2.59
C-3	4	8.00	3.6	2.00	1.11

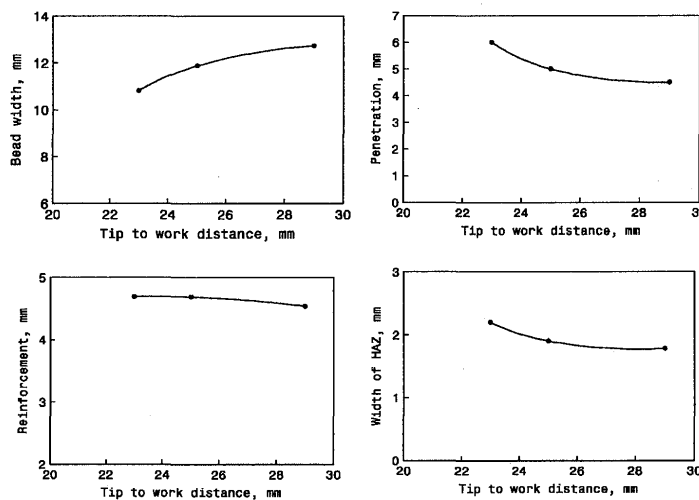


Fig.1 Effect of tip to work distance on weld bead geometry as well as on the HAZ widths in Ar shielding gas.

Effect of Welding Parameters of FCAW Process and Shielding Gas Type on Weld Bead Geometry and Hardness Distribution

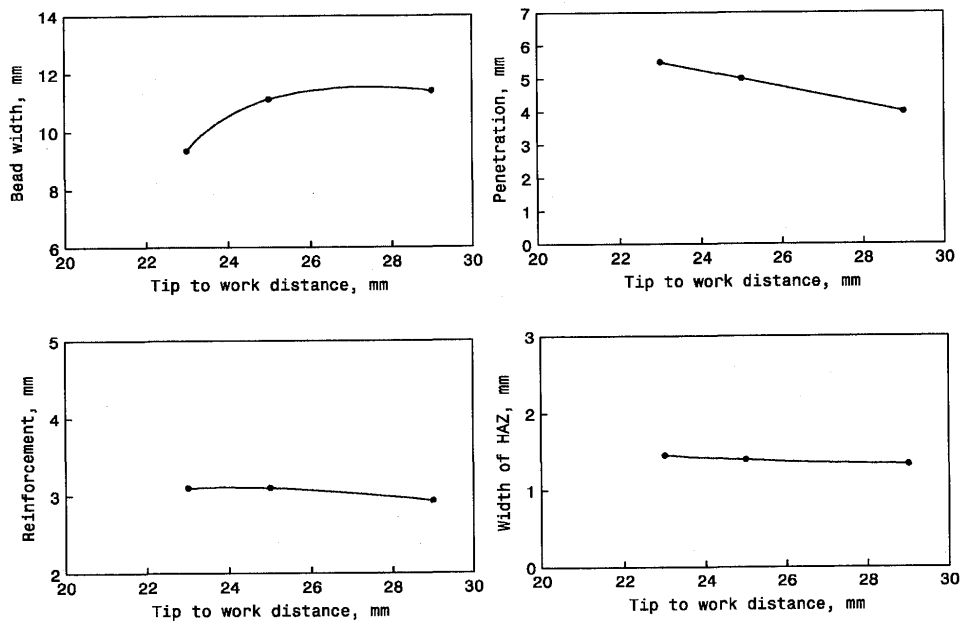


Fig. 2 Effect of tip to work distance on weld bead geometry as well as on the HAZ widths in CO₂ shielding gas.

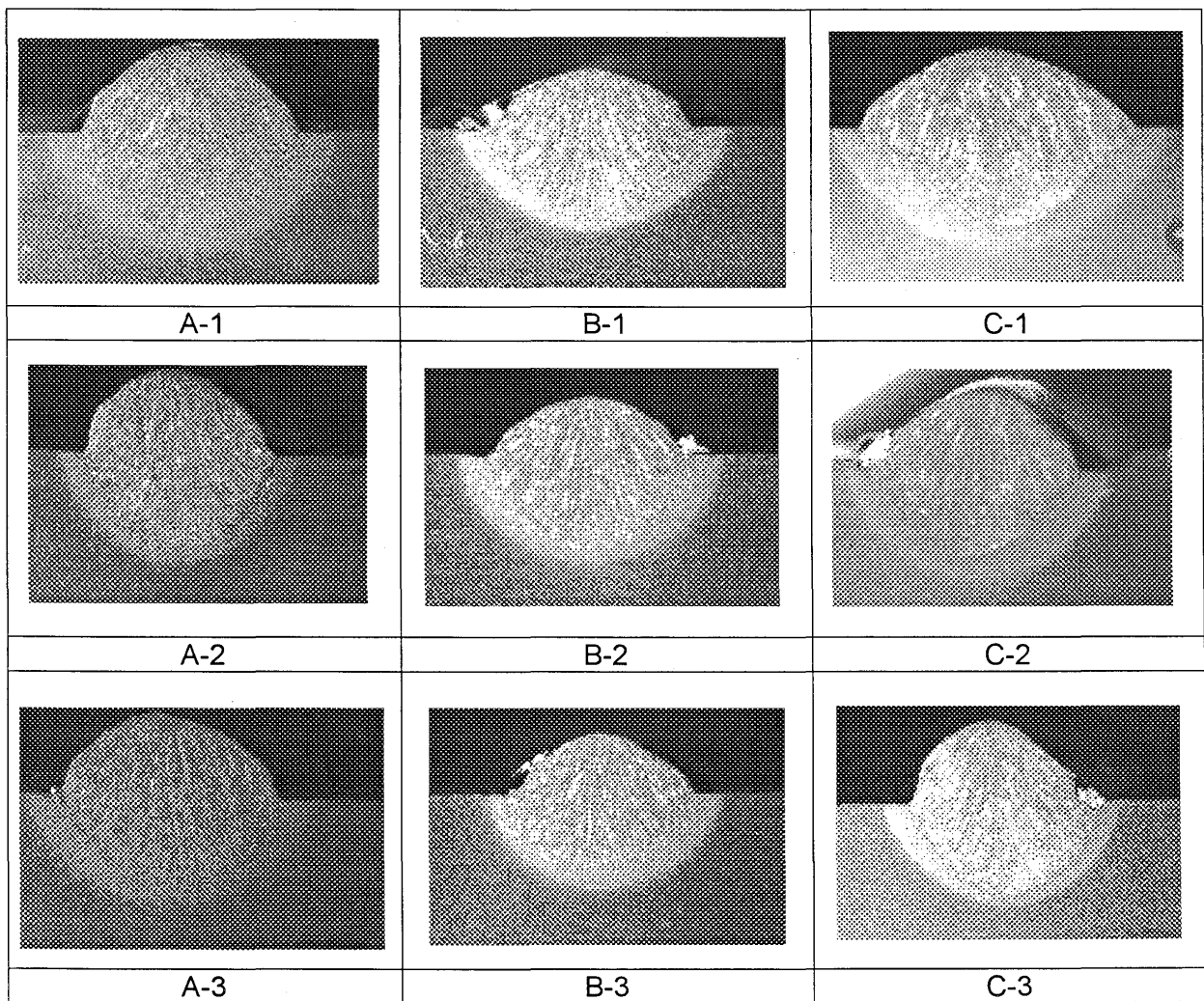


Fig. 3 Macrostructure of the investigated samples at different welding parameters and shielding gases.

Within this range and from the results shown in Table 3, it can be concluded that the best welding parameters can be achieved by the welding conditions used in the samples A-1 and B-2, from the view point of weld bead geometry. However, the width of HAZ is another important factor that has to be considered.

3.2 Effect of tip to work distance on heat affected zone width

The width of the heat affected zone was measured for different tip to work distance and different shielding gases. The results are shown in Fig.1, 2&3 respectively. The width of the heat affected zone is decreased with the increase in tip to work distance. This can be attributed to the decrease of heat, which transferred from the arc column to the base metal due to the reduction of arc column size and redistribution of plasma stream inside the arc, with increasing tip to work distance ¹⁾.

3.3 Effect of welding travelling speed on weld bead geometry and HAZ width

The weld bead geometry and HAZ width were measured

at different welding travelling speeds and constant tip to work distance in pure Ar. The results are tabulated in Table 3 and shown in Fig.4. The photographs of macrostructure are shown in Fig.3.

With increasing welding travelling speed, weld metal cross sectional area (bead geometry) and HAZ width will be reduced. This can be related to the decrease in amount of heat input with increasing welding travelling speed.

3.4 Hot cracking test

Low alloy steels are prone to hot cracking and particularly to solidification cracking. Examination of the restraint test samples by dye pentrant test and optical microscopy showed that solidification cracks occasionally occurred as in case of specimens A-1, C-1, C-2 and H-4 while no cracks were found when using the other weld conditions. The reasons are partly due to the metallurgical microstructures, heat input and the amount of residual stresses. Accordingly, at lower heat input the amount of segregation produced, such as low melting elements like P and S or low melting carbide phases, is smaller than that obtained at higher heat input. Therefore, cracking response

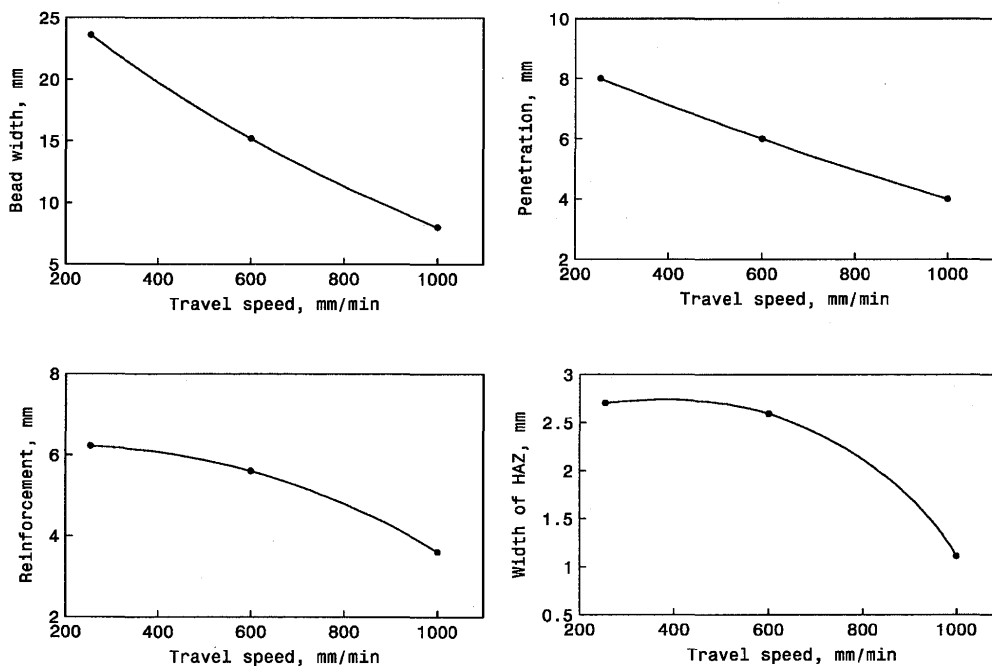


Fig.4 Effect of welding travelling speed on weld bead geometry as well as on the HAZ width, at constant tip to work distance in Ar shielding gas.

Effect of Welding Parameters of FCAW Process and Shielding Gas Type on Weld Bead Geometry and Hardness Distribution

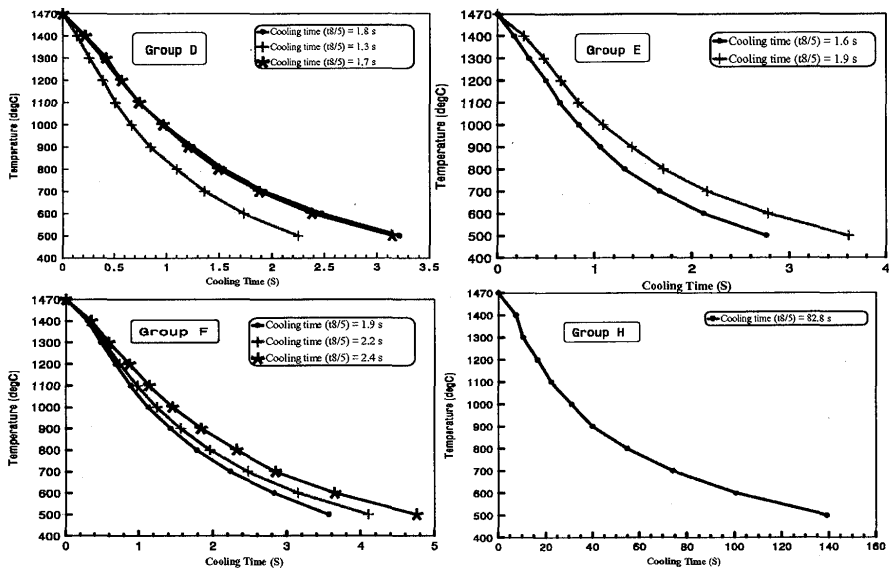


Fig.5 Cooling time as a function of different welding currents at constant welding voltage and traveling speed

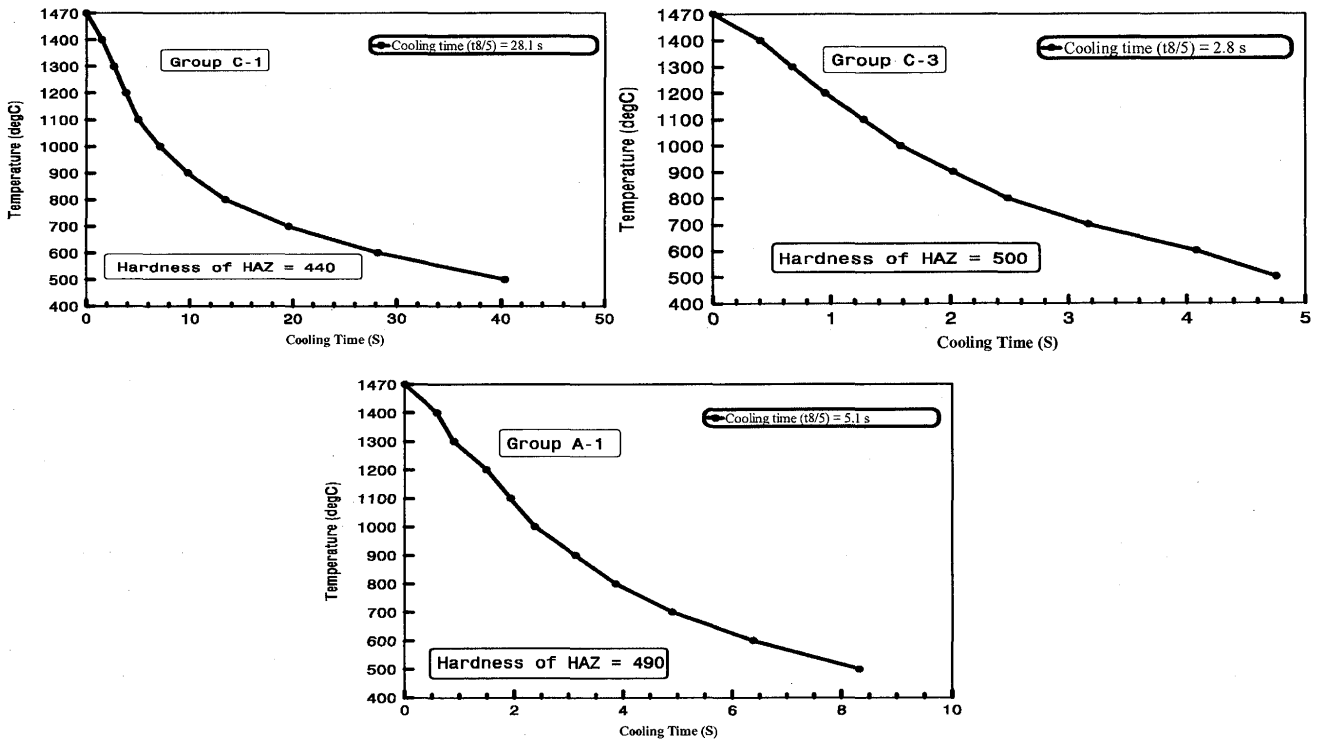


Fig. 6 Cooling time as function of different welding speeds at constant welding current and voltage

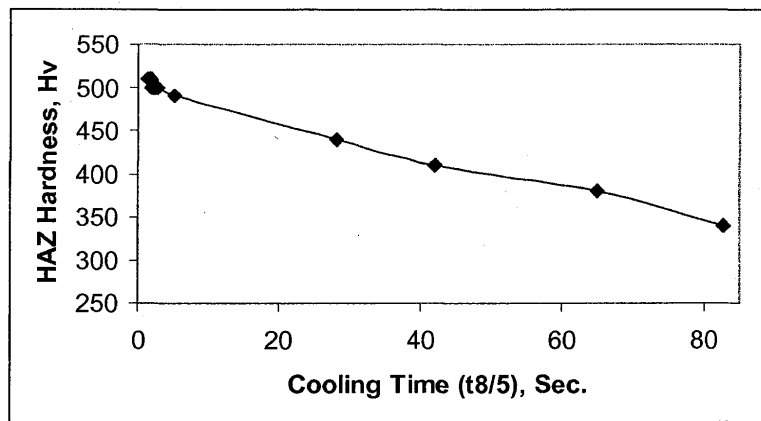


Fig.7 Effect of cooling time on the hardness of heat affected zone

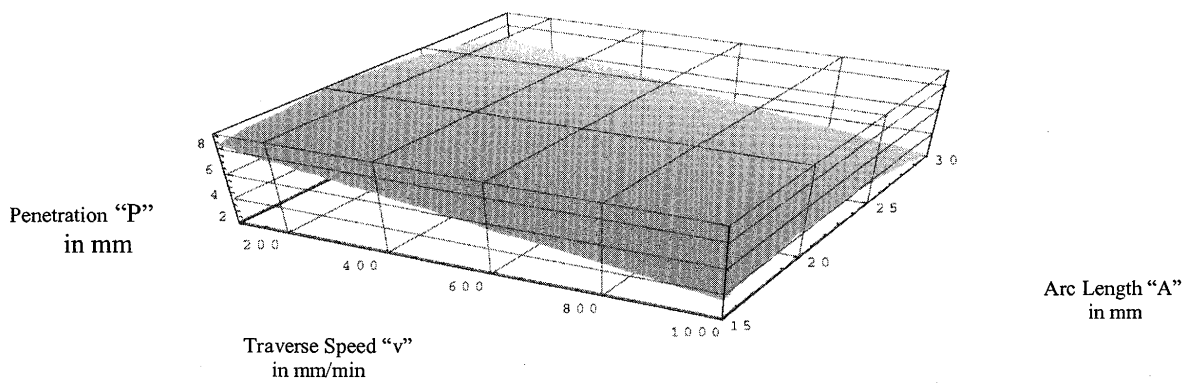


Fig. 8 Relationship between welding travelling speeds (v), tip to work distance (a) and penetration (a).

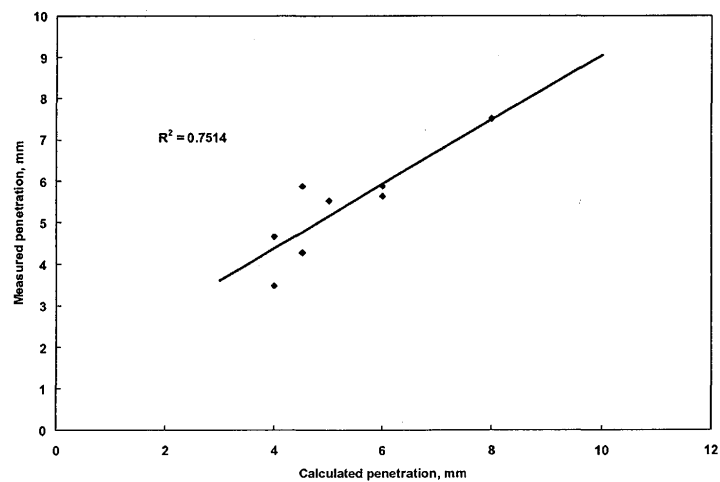


Fig.9 Relationship between the measured and calculated values of penetration

in the latter case will be higher due to the changes of weld pool shape and to the increase in heat input. High heat input leads to lower cooling rate, wider liquidus-solidus range, coarser cell size and high amount of segregation, as well as the change in stress distribution along the weldment as a function of temperature gradient around the weld pool²⁾.

3.5 Effect of cooling time on hardness of HAZ

The measured cooling time curves are shown in Fig. 5 as a function of different welding current at constant welding voltage and traveling speed, while the results shown in Fig.6 are measured at different welding speeds at constant welding current and voltage. Special consideration was given to the cooling rate from 800 to 500 °C, during solidification, and the measured cooling rate is also shown. The hardness of the HAZ as a function of cooling time is shown in Fig.7.

From these results the following points were concluded:

1. The effect of welding current on the hardness of HAZ is small when other welding variables are constant.
2. The welding speed has the biggest effect on the cooling time as well as on the hardness value of the HAZ. At lower welding speeds, the amount of adjacent material affected by the heat of the arc is increased, resulting in a wider HAZ, as shown in Fig.7, slower cooling rate, and lower hardness value. However, the amount of residual stresses will be increased resulting an increase in the susceptibility to hot cracking. This corresponds with the previous results on hot cracking. However, at higher welding speeds the amount of adjacent material affected by the heat of the arc is reduced, resulting in the decreasing of residual stresses and increasing of HAZ hardness of this type of steel. Noting that for this steel type, the A_{c1} -temperature is about 708 °C, with the A_{c3} -temperature of 849 °C and M_s of 370 °C.
3. At higher levels of welding current and voltage the effect of welding speed and cooling time on the hardness values is relatively remarkable, as shown in Fig.6 (C-1&C-3), but still higher than the acceptable range stated in ASME section VIII.
4. The effect of welding voltage on the hardness of HAZ is also small when other welding variables are constant.

3.6 Mathematical modelling

By curve fitting to the experimental results, a mathematical relationship between the depth of penetration, d , (an output) and welding travelling speed, v ,

and the tip to work distance, a , (as inputs) can be calculated as follows:

$$d = -0.0054 v + 0.93 a - 0.023 a^2$$

The above empirical equation can be plotted as shown in Fig.8.

Figure 9 shows the relationship between the calculated and measured values of weld bead penetration at different values of the welding variables. It can be said that the values calculated by the empirical equation are in good agreement with the actual values.

4. Conclusions

The effects of welding variables on the weld bead geometry and the width of HAZ have been investigated and discussed. Also, an empirical formula developed from two welding variables was introduced to estimate the amount of penetration.

The following specific conclusions can be drawn from the results of this study:

1. With increasing tip to work distance, the bead width increases and the reinforcement and penetration decrease.
2. The measured values of weld bead dimensions are generally higher for the case of Ar gas shielding than in the case of CO₂ gas shielding.
3. The width of heat affected zone decreases with an increase in tip to work distance.
4. With increasing welding travelling speed, weld metal cross sectional area and HAZ width will be reduced. On the other hand, the hardness of HAZ will be increased.

This work will be extended to get an appropriate hardness prediction formula and another empirical formula based on base metal chemical composition and weld cooling time. Combined with the formula in this paper methods will be developed for determining the welding procedure needed to achieve a specific maximum HAZ hardness or estimating the HAZ hardness of existing welds. This will be extended to temper bead welding for repair welding.

References

- 1) J.F. Lancaster *The physics of welding*, IAWQ Pergamon Press, Oxford 1984
- 2) Dolby, "Factors Controlling Weld Toughness-The Present Position", Part 2, Weld Metals, Weld. Inst. Res. Rep., 14/1976M.